International Journal of Control, Automation and Systems 15(1) (2017) 404-415
http://dx.doi.org/10.1007/s12555-015-0181-1
ISSN:1598-6446 eISSN:2005-4092
http://www.springer.com/12555

Neural Network Based Adaptive Fuzzy PID-type Sliding Mode Attitude Control for a Reentry Vehicle

Zhen Jin, Jiabin Chen*, Yongzhi Sheng, and Xiangdong Liu

Abstract: This work investigates the attitude control of reentry vehicle under modeling inaccuracies and external disturbances. A robust adaptive fuzzy PID-type sliding mode control (AFPID-SMC) is designed with the utilization of radial basis function (RBF) neural network. In order to improve the transient performance and ensure small steady state tracking error, the gain parameters of PID-type sliding mode manifold are adjusted online by using adaptive fuzzy logic system (FLS). Additionally, the designed new adaptive law can ensure that the closed-loop system is asymptotically stable. Meanwhile, the problem of the actuator saturation, caused by integral term of sliding mode manifold, is avoided even under large initial tracking error. Furthermore, to eliminate the need of a priori knowledge of the disturbance upper bound, RBF neural network observer is used to estimate the disturbance information. The stability of the closed-loop system is proved via Lyapunov direct approach. Finally, the numerical simulations verify that the proposed controller is better than conventional PID-type SMC in terms of improving the transient performance and robustness.

Keywords: Actuator saturation, adaptive fuzzy PID-type SMC, attitude control, radial basis function neural network, reentry vehicle.

1. INTRODUCTION

Reentry vehicle is sensitive to changes in flight conditions, aerodynamic characteristics, and physical parameters because of its broad flight envelope spanning and flight condition of high Mach numbers [1]. As a result, the model of the reentry vehicle is highly nonlinear and time-varying, with modeling inaccuracies and external disturbances [2]. These problems have strong adverse in- fluences on the performance of reentry vehicle and add the difficult in design of the control system. Therefore, many robust control algorithms, such as H, sliding mode control (SMC), and adaptive control have been used for reentry vehicle [3–6, 11].

Over the past decade, the sliding mode control, as one of the most significant robust control methods, provides a systematic approach to the nonlinear system with modeling inaccuracies and external disturbances under matching conditions [7–9]. Hence, SMC has been widely used for the reentry vehicle attitude control [10, 11]. In [10], a quasi-continuous high-order sliding mode control law with feedback linearization (FBL) was proposed for a flexible air-breathing hypersonic vehicle (FAHV). In [11], a robust adaptive SMC design method for the longitudinal model of FAHV with parameter uncertainties and external disturbances was proposed, by which the system without the prior knowledge of disturbances upper-bound is considered.

In the conventional SMC design, the chattering, which may trigger unmodeled high-frequency dynamic [12], must be addressed. The boundary layer technique [13], as the main method to eliminate the chattering, has been adopted in many papers. However, the robustness and accuracy of the control system will not be guaranteed within the boundary layer. Contraposing this problem, the constant PID-type sliding mode control (CPID-SMC) was presented in [14], adding an integral term to the conventional PD sliding mode manifold, which has proved that the less steady state error can be achieved. But it will deteriorate the transient performance of the system [15]. In particular, it would lead to instable situation of system with constraint of control input due to integral windup effect.

To deal with the problem of CPID-SMC, some studies have been done in references [16, 17]. In [16], the authors selected a small integral terms gain to avoid input saturation and overshoot of the system, but it would sacrifice the response rapidity of system. In [17], the authors incorpo-

Manuscript received April 26, 2015; revised November 14, 2015 and November 14, 2015; accepted December 31, 2015. Recommended by Associate Editor Yingmin Jia under the direction of Editor Euntai Kim. This work is supported by National Natural Science Foundation of China under grant 11402020 and 11372034, Innovative Research Team of Beijing Institute of Technology.

Zhen Jin, Jiabin Chen, Yongzhi Sheng, and Xiangdong Liu are with School of Automation, Key laboratory for Intelligent Control & Decision of Complex Systems, Beijing Institute of Technology, Beijing, 100081, China (e-mails: jinzhen0904@163.com, jiabinc_ice_fire@163.com, {shengyongzhi, xdliu}@bit.edu.cn).
* Corresponding author.

rated a conditional integrator, providing integral action only inside the boundary layer. The essence of the method is that the integral term would only work in some specific areas, and it is effective to decrease system response overshoot. In this paper, we will consider this problem from a difference aspect.

The prior knowledge of matched disturbances upper bound is necessary for SMC. However, it cannot be obtained in the actual system. To ensure the stability of the system, one solution is to select a large switching gain, which as a result may lead to more exquisite chatteting phenomenon. To solve this problem, in [18], adaptive control method is applied, in which the gain dynamics ensure that there is no over-estimation of the gain with respect to the real a priori unknown value of disturbances, and the controller chattering phenomenon is resolved. Besides, observer technology, such as super-twisting algorithm [19] and neural network [20,21] are also adopted to estimate upper bound information of the unknown disturbances. But super-twisting algorithm still requires prior knowledge of the disturbances. As the observer, neural network is applied to the sliding mode control. In [22], neural network is utilized to estimate the modeling inaccuracies and external disturbances of linear system online, by which the chattering phenomenon can be eliminated. In [23], an adaptive sliding mode control with neural network is proposed for a discrete nonlinear system, and the neural network is used to approximate unknown functions. Compared with [18], neural network observer can also enhance the system robustness except for estimating the unknown disturbances.

In this paper, to overcome the aforementioned two problems of CPID-SMC, an adaptive fuzzy PID-type sliding mode control based on RBF neural network is proposed.

The main contributions of this study are as follows:

1) In our paper, the adaptive fuzzy logic system is utilized to tackle transient response problem. Different from [24], in which fuzzy logic system without adaptive law was used to tuning the PID control parameters for improving the system performances, in this paper, a new adaptive law is designed for the fuzzy logic system to adjust the gain parameters of sliding mode manifold. The principle of the designing of adaptive fuzzy algorithm is that the large errors correspond to small gains and the small errors correspond to large gains. Then the problem of the actuator saturation, caused by integral term of sliding mode manifold, is also avoided.

2) The adaptive RBF neural network is designed as disturbance observer to estimate the matched lumped disturbances . The RBF neural network observer is not only able to estimate the disturbances information, but also avoids the need for prior knowledge of disturbance upper bound. Meanwhile, the superior properities, such as higher precision and robustness against disturbances, are achieved.

3) Although many states are considered in the system, only three parameters are required to be adapted online in fuzzy logic system and neural network. Thus the computation load of the proposed controller can be reduced, and it can be applied in practice possiblly.

The paper is organized as follows. In Sections 2 and 3, the reentry vehicle mathematical model is described, the FBL model of the vehicle and control objective are presented. Then we review the CPID-SMC, and discuss its characteristics and problems. The FLS and AFPID-SMC are proposed for the attitude control of reentry vehicle with modeling inaccuracies and external disturb- ances, in addition, the stability of the closed-loop system is also proved based on Lyapunov Theory in Section 4. Then Section 4 also develops the adaptive RBF neural network observer to approximate unknown disturbances. Numerical simulations are presented in Section 5. Finally, the conclusions are summarized in Section 6.

2. MATHEMATICAL MODEL AND PROBLEM FORMULATION

In this section, the feedback linearization method is used to linearize the dynamics of the reentry vehicle system.

2.1. Mathematical model

The dynamic equations of related rotational model of the reentry vehicle is described as cite25:

$$\begin{aligned} &\dot{\Omega} = T(\Omega)\omega + \Delta T, \\ &I\dot{\omega} + \omega^{\times} I\omega = M + M_d, \end{aligned} \tag{1}$$

where

$$\Omega = [\alpha, \beta, \mu]^T,$$

$$T(\Omega) = \begin{bmatrix} -\cos\alpha\tan\beta & 1 & -\sin\alpha\tan\beta \\ \sin\alpha & 0 & -\cos\alpha \\ -\cos\alpha\cos\beta & -\sin\beta & -\sin\alpha\cos\beta \end{bmatrix},$$

$$I = \begin{bmatrix} I_{xx} & 0 & -I_{xz} \\ 0 & I_{yy} & 0 \\ -I_{xz} & 0 & I_{zz} \end{bmatrix},$$

$$\omega = [p, q, r]^T,$$

$$\omega^{\times} = \begin{bmatrix} 0 & -\omega_z & \omega_y \\ \omega_z & 0 & -\omega_x \\ -\omega_y & \omega_x & 0 \end{bmatrix},$$

$$M = [M_x, M_y, M_z]^T,$$

$$M_d = [M_{dx}, M_{dy}, M_{dz}]^T,$$

$$\Delta T = [\Delta T_1, \Delta T_2, \Delta T_3]^T,$$

$\Omega = [\alpha, \beta, \mu]^T$ is the angular vector, α, β, μ stand for attack angle, sideslip angle, and bank angle respectively. $\omega = [p, q, r]^T$ is the angular rate vector defined as roll, pitch, and yaw rates. $M = [M_x, M_y, M_z]^T$ denotes the vector

of control moment with M_x, M_y, M_z being the roll, pitch and yaw moments respectively. I is the inertia matrix. $M_d = [M_{dx}, M_{dy}, M_{dz}]^T$ is the bounded unknown external disturbance moment. $\Delta T = [\Delta T_1, \Delta T_2, \Delta T_3]^T$ denotes the bounded unknown modeling inaccuracies.

2.2. Feedback linearization (FBL) model

The dynamic equations of reentry vehicle described by (1) can be rewritten as follows:

$$\begin{aligned} \dot{x} &= f(x) + \sum_{k=1}^{3} g_k(x) u_k + \Delta f, \\ y_i &= h_i(x) \qquad i = 1,2,3, \end{aligned} \tag{2}$$

where $x = [\alpha, \beta, \mu, p, q, r]^T$ is the state vector, $u = [u_1, u_2, u_3]^T = [M_x, M_y, M_z]^T$ and $y = [y_1, y_2, y_3] = h(x) = [\alpha, \beta, \mu]^T$ denote the vectors of control input and output respectively, and $f(x)$, $g(x)$ are smooth functions in R^n:

$$\begin{aligned} f(x) &= \begin{bmatrix} f_1(x) & f_2(x) & f_3(x) & f_4(x) & f_5(x) & f_6(x) \end{bmatrix}^T \\ &= \begin{bmatrix} -p\cos\alpha\tan\beta + q - r\sin\alpha\tan\beta \\ p\sin\alpha - r\cos\alpha \\ -p\cos\alpha\cos\beta - q\sin\beta - r\sin\alpha\cos\beta \\ \dfrac{(I_{xx} - I_{yy} + I_{zz})I_{xz}}{I^*} pq + \dfrac{(I_{yy} - I_{zz})I_{zz} - I_{xz}^2}{I^*} qr \\ \dfrac{I_{xz}}{I_{yy}}(r^2 - p^2) + \dfrac{I_{zz} - I_{xx}}{I_{yy}} pr \\ \dfrac{(I_{xx} - I_{yy})I_{xx} + I_{xz}^2}{I^*} pq + \dfrac{(-I_{xx} + I_{yy} - I_{zz})I_{xz}}{I^*} qr \end{bmatrix}, \end{aligned}$$

$$g_1(x) = \left[0, 0, 0, \frac{I_{zz}}{I^*}, 0, \frac{I_{xz}}{I^*}\right]^T,$$

$$g_2(x) = \left[0, 0, 0, 0, \frac{1}{I_{yy}}, 0\right]^T,$$

$$g_3(x) = \left[0, 0, 0, \frac{I_{xz}}{I^*}, 0, \frac{I_{xx}}{I^*}\right]^T,$$

where $I^* = I_{xx}I_{zz} - I_{xz}^2$. Δf denotes the unknown external disturbances.

Applying the FBL technique [26] to the rotational model (2) of the reentry vehicle, we can calculate the differential of the each output until the control inputs appear in the final equations. The final equations can be obtained by differentiating twice to each output y_i. The output dynamic for y is described as

$$\begin{aligned} \begin{bmatrix} \ddot{y}_1 \\ \ddot{y}_2 \\ \ddot{y}_3 \end{bmatrix} &= \underbrace{\begin{bmatrix} L_f^2(h_1) \\ L_f^2(h_2) \\ L_f^2(h_3) \end{bmatrix}}_{F} \\ &+ \underbrace{\begin{bmatrix} L_{g1}(L_f h_1) & L_{g2}(L_f h_1) & L_{g3}(L_f h_1) \\ L_{g1}(L_f h_2) & L_{g2}(L_f h_2) & L_{g3}(L_f h_2) \\ L_{g1}(L_f h_3) & L_{g2}(L_f h_3) & L_{g3}(L_f h_3) \end{bmatrix}}_{E} M + \Delta\nu \\ &= F + EM + \Delta n u, \end{aligned} \tag{3}$$

where $\Delta\nu = [\Delta\nu_1, \Delta\nu_2, \Delta\nu 3]$ denotes the lumped disturbances resulted from the linearization procedure. From equation (3), we can know that the relative degree of the reentry vehicle, $l = 2+2+2 = 6 = n$, equals to the dimension of the system. Thus, the nonlinear system (2) can be linearized completely.

Furthermore, by calculating, one gets

$$\det(E) = \frac{\cos\beta}{I * I_{yy}} - \frac{\sin\beta\tan\beta}{I * I_{yy}} \approx \frac{\cos\beta}{I * I_{yy}} \neq 0,$$

where sideslip angle β can be considered as 0 during the reentry phase.

Due to the nonsingular input matrix , the feedback control law can be defined as

$$M = E^{-1}(-F + \nu), \tag{4}$$

and

$$\ddot{y} = \nu + \Delta\nu, \tag{5}$$

where $\nu = [\nu_1, \nu_2, \nu_3]^T$ denotes the assistant control input.

Assumption 1: The aggregate disturbances $\Delta\nu_i$ are assumed to be bounded by known constants:

$$|\Delta\nu| \leq l_d, \quad l_d = \max\{\Delta\nu_1, \Delta\nu_2, \Delta\nu_3\};$$

where $l_d > 0$ is a known constant.

2.3. Control object

In this paper, the target of the attitude control design is to determine the control moment vector M to guarantee that the output vector $y = [\alpha, \beta, \mu]^T$ tracks the command signals $y_c = [\alpha_c, \beta_c, \mu_c]^T$ asymptotically with external disturbances and modeling inaccuracies, i.e.,

$$\lim_{t\to\infty} e = \lim_{t\to\infty}(y - y_c) = 0, \tag{6}$$

where $e = [e_1, e_2, e_3]^T = [y - y_c]^T = [\alpha - \alpha_c, \beta - \beta_c, \mu - \mu_c]^T$ is the tracking error vector.

3. CONSTANT PID-TYPE SLIDING MODE CONTROL (CPID-SMC)

In this section, the conventional CPID-type sliding mode control and its principle are reviewed.

Firstly, for the attitude system of reentry vehicle (5), the CPID-type sliding mode manifold $S = [s_1, s_2, s_3]^T$ is designed as [27]:

$$S = \dot{e}(t) + K_p e(t) + K_I \int_0^t e(t)dt, \tag{7}$$

where the parameters $K_P = diag(k_{p1}, k_{p2}, k_{p3})$ and $K_I = diag(k_{i1}, k_{i2}, k_{i3})$ are the design parameters to ensure the errors of the attitude angles can converge to zero on $S = 0$.

Once the sliding mode manifold is established with a proper controller, the dynamic of the CPID-type sliding mode can be obtained by:

$$\ddot{e}(t)+K_P\dot{e}(t)+K_I e(t)=0. \tag{8}$$

With (8) and the design principle of sliding mode control, the CPID-type sliding mode control for reentry vehicle system (5) can be acquired as follows:

$$v=\ddot{y}_c-K_P\dot{e}(t)-K_I e(t)-\eta \mathrm{sgn}(S), \tag{9}$$

where $\eta=diag(\eta_1,\eta_2,\eta_3)$ is the switching gain matrix and its elements satisfy $\eta_i \geq l_d+\ell$ with being an arbitrary positive constant. The $\mathrm{sgn}(\cdot)$ denotes sign function, i.e., $\mathrm{sgn}(S)=[\mathrm{sgn}(s_1),\mathrm{sgn}(s_2),\mathrm{sgn}(s_3)]^T$.

Because (8) is a typical second-order system, it can be concluded that the attitude tracking error e is asymptotically stable. Moreover, it has denoted that less steady state error can be achieved due to the existing of integral term in sliding mode manifold. However, from (8), we can know that the large gains can cause control saturation and response overshoot of the system but ensure small static errors and fast response. Meanwhile, small gains can eliminate control saturation and response overshoot of the system but will lose the advantages of small static errors and fast response. These contradictions are caused by the characteristic of the sliding mode manifold dynamic of CPID-SMC.

4. NEURAL NETWORK BASED ADAPTIVE FUZZY PID-TYPE SLIDING MODE CONTROL

In this section, AFPID-SMC-RBF is presented and the adaptive laws are developed based on the Lyapunov Theory.

The block configuration of overall scheme of reentry vehicle is presented in Fig. 1. In this figure, it can be seen that the overall scheme consists of two parts: adaptive fuzzy sliding mode controller and neural network observer. The fuzzy logic system is applied to improve the transient performance and avoid control saturation. Then the need for prior knowledge of disturbances upper bound is avoided by neural network which meanwhile enhances the the system robustness.

4.1. Adaptive Fuzzy Logic System (AFLS)

As shown in Fig. 2, which presents the basic block configuration of the adaptive fuzzy logic system, an AFLS is composed of five principal components: fuzzier, fuzzy rule base, inference engine, defuzzifier and adaptive law. The five parts of a fuzzy system decide a MIMO structure: $U \in R^m \rightarrow R^n$, where U is a compact set. In this paper, $\|e\|^2$ and $\|\dot{e}\|^2$, which characterize the degree of the departure from the equilibrium point $(e,\dot{e})=(0,0)$, are the input of the AFLS. The parameters and are the outputs of the AFLS.

The fuzzifier maps the detected crisp input space U into the fuzzy sets defined in U. And the defuzzifier performs a reverse function to map fuzzy sets in R into a crisp point in R [28]. The fuzzy rule base consists of a set of fuzzy rules based upon "IF-THEN." Correspondingly, the fuzzifier maps an observed crisp point $(e,\dot{e})$ into the fuzzy sets F_1^j, F_2^j in U. The fuzzy rule base and inference engine perform a mapping from fuzzy sets of input F_1^j, F_2^j to fuzzy sets of output A_1^j, A_2^j. The defuzzifier maps the fuzzy sets A_1^j, A_2^j to a crisp point (K_{AP},K_{AI}).

The fuzzy rule base consists of M rules as follows:

$$\begin{aligned} &R^j\text{: IF } \|e\|^2 \text{ is } F_1^j \text{ and } \|\dot{e}\|^2 \text{ is } F_2^j\text{, THEN } K_{AP} \text{ is} \\ &A_1^j \text{ and } K_{AI} \text{ is } A_2^j. \qquad j=1,2,...,M, \end{aligned} \tag{10}$$

where F_1^j, f_2^j, $A-1^j$, A_2^j are fuzzy sets corresponding to $\|e\|^2$, $\|\dot{e}\|^2$, K_{AP}, K_{AI}.

Each fuzzy rule IF-THEN of(10) defines two fuzzy applications $F_1^j \times F_2^j \rightarrow A_1^j$, $F_1^j \times F_2^j \rightarrow A_2^j$. And the membership functions of F_1^j, F_2^j, A_1^j, A_2^j are expressed by $\mu_{F_1^j}$, $\mu_{F_2^j}$, $\mu_{A_1^j}$ and $\mu_{A_2^j}$.

In this paper, the FLS is designed by using singleton fuzzifier, product inference, center average defuzzifier, so K_{AP}, K_{AI} can be written as linear combinations of fuzzy basis functions as follows [29]:

$$\begin{aligned} K_{AP} =& f_1(\|e\|^2,\|\dot{e}\|^2)=\frac{\sum_{j=1}^M \bar{k}_P^j \mu_{F_1^j}(\|e\|^2)\mu_{F_2^j}(\|\dot{e}\|^2)}{\sum_{j=1}^M \mu_{F_1^j}(\|e\|^2)\mu_{F_2^j}(\|\dot{e}\|^2)} \\ =& \kappa_1 \mathcal{G}(\|e\|^2,\|\dot{e}\|^2), \end{aligned} \tag{11a}$$

$$\begin{aligned} K_{AI} =& f_2(\|e\|^2,\|\dot{e}\|^2)=\frac{\sum_{j=1}^M \bar{k}_I^j \mu_{F_1^j}(\|e\|^2)\mu_{F_2^j}(\|\dot{e}\|^2)}{\sum_{j=1}^M \mu_{F_1^j}(\|e\|^2)\mu_{F_2^j}(\|\dot{e}\|^2)} \\ =& \kappa_2 \mathcal{G}(\|e\|^2,\|\dot{e}\|^2), \end{aligned} \tag{11b}$$

where $\bar{k}_p^j$, $\bar{k}_i^j$ are the points at which $\mu_{A_1^j}$ and $\mu_{A_2^j}$ achieve their maximum value, and

$$\begin{aligned} \kappa_1 &= (\bar{k}_P^1,\bar{k}_P^2,...,\bar{k}_P^M), \\ \kappa_2 &= (\bar{k}_I^1,\bar{k}_I^2,...,\bar{k}_I^M), \end{aligned} \tag{12}$$

are adjustable parameter vectors. $\mathcal{G}(\|e\|^2,\|\dot{w}\|^2)$ is the fuzzy basis function vector, and its elements are given by:

$$\mathcal{G}^j(\|e\|^2,\|\dot{e}\|^2)=\frac{\mu_{F_1^j}(\|e\|^2)\mu_{F_2^j}(\|\dot{e}\|^2)}{\sum_{j=1}^M \mu_{F_1^j}(\|e\|^2)\mu_{F_2^j}(\|\dot{e}\|^2)}. \tag{13}$$

In this paper, the Gaussian membership function is applied to implement the adaptive fuzzy logic system. The expressions of all membership functions can be defined by:

$$\mu_\chi^j(\nabla)=\exp\left(-\left(\frac{\nabla-c_\chi^j}{\sigma\chi}\right)^2\right), \tag{14}$$

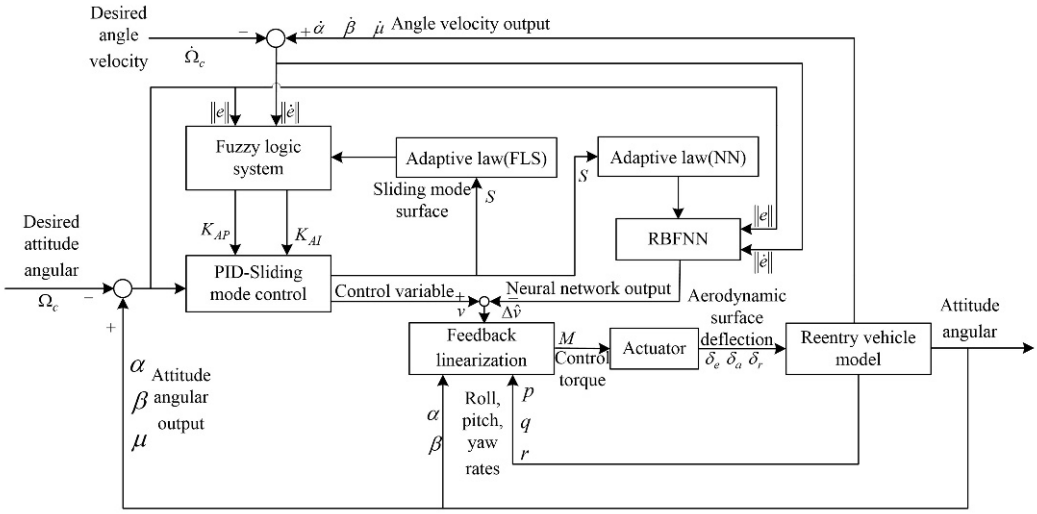

Fig. 1. Block configuration of overall scheme of reentry vehicle.

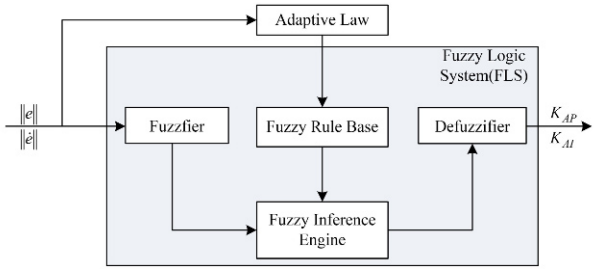

Fig. 2. Basic block configuration of the adaptive fuzzy logic system.

where ∇ denotes $\|e\|^2$ or $\|\dot{e}\|^2$, χ denotes F_1^j and F_2^j. c_χ^j, σ^χ are elements of vectors c, σ.

4.2. Adaptive fuzzy PID-type sliding mode control law

The main idea of AFPID-SMC is that gains of the sliding mode manifold are adjusted online by the adaptive fuzzy block designed in Section 4.1. The principle of adaptive fuzzy logic system is that the large errors correspond to small gains and the small errors correspond to large gains. To ensure the stability of the closed-loop system, the adaptive update laws of κ_1, κ_2 are given by:

$$\begin{aligned}\dot{\bar{k}}_P^j &= -\frac{r_1 g_{P_j} S^T S}{\bar{k}_P^j}\frac{\mu_{F_1^j}(\|e\|^2)\mu_{F_2^j}(\|\dot{e}\|^2)}{\sum_{j=1}^M \mu_{F_1^j}(\|e\|^2)\mu_{F_2^j}(\|\dot{e}\|^2)} \\ &= -\frac{r_1 g_{P_j} S^T S}{\bar{k}_P^j}\mathcal{G}, \\ \dot{\bar{k}}_I^j &= -\frac{r_2 g_{I_j} S^T S}{\bar{k}_I^j}\frac{\mu_{F_1^j}(\|e\|^2)\mu_{F_2^j}(\|\dot{e}\|^2)}{\sum_{j=1}^M \mu_{F_1^j}(\|e\|^2)\mu_{F_2^j}(\|\dot{e}\|^2)} \\ &= -\frac{r_2 g_{I_j} S^T S}{\bar{k}_I^j}\mathcal{G},\end{aligned} \tag{15}$$

where r_1, r_2, g_{P_j} and g_{I_j} are positive constants.

Using the adaptive fuzzy logic system, the AFPID-type sliding mode manifold $S-[s_1,s_2,s_3]^T$ is designed as follows:

$$S = \dot{e}(t) + \int_0^t K_{AP}\dot{e}(t)dt + \int_0^t K_{AI}e(t)dt, \tag{16}$$

where the proportional gain parameter vector $K_{AP} = diag(k_{Ap1}, k_{Ap2}, k_{Ap3})$ and integral gain vector $K_{AI} = diag(k_{Ai1}, k_{Ai2}, k_{Ai3})$, are tuned by the AFLS online.

According to (16), the adaptive controller is designed as follows:

$$v = \ddot{y}_c - K_{AP}\dot{e}(t) - K_{AI}e(t) - \eta\,\mathrm{sgn}(S), \tag{17}$$

where η is selected in the same way as that in (9).

The proportional gain K_{AP} and integral gain K_{AI} of the controller (17) are adjusted by adaptive fuzzy logic system. In order to achieve the expected transient performance, the gains should be set as small values when the tracking error is large, and the gains gradually increase as tracking errors decrease. Finally, the transient performances of the system is kept by this regulation strategy.

Theorem 1: Consider the reentry vehicle system (5) with the sliding mode manifold defined by (16), and the Assumption 1 is met. The adaptive fuzzy sliding mode control (17) with the adaptive law (15) can ensure that the attitude tracking error e is asymptotically stable.

Proof: Consider the following Lyapunov candidate function:

$$V_1 = \frac{1}{2}S^T S + \frac{1}{2r_1}\kappa_1\kappa_1^T + \frac{1}{2r_2}\kappa_2\kappa_2^T. \tag{18}$$

The time derivative of V_1 is given by:

$$\dot{V}_1 = S^T\dot{S} + \frac{1}{r_1}\dot{\kappa}_1\kappa_1^T + \frac{1}{r_2}\dot{\kappa}_2\kappa_2^T$$

$$
\begin{aligned}
&=S^T(\ddot{e}(t)+K_{AP}\dot{e}(t)+K_{AI}e(t)\\
&\quad+\frac{1}{r_1}\dot{\kappa}_1\kappa_1^T+\frac{1}{r_2}\dot{\kappa}_2\kappa_2^T \qquad (19)\\
&=S^T(\nu+\Delta\nu-\ddot{y}_c+K_{AP}\dot{e}(t)+K_{AI}e(t))\\
&\quad+\frac{1}{r_1}\dot{\kappa}_1\kappa_1^T+\frac{1}{r_2}\dot{\kappa}_2\kappa_2^T.
\end{aligned}
$$

Substituting the controller (17) and adaptive law (15) in (19), one gets:

$$
\begin{aligned}
\dot{V}_1 =&S^T(\ddot{y}_c-K_{AP}\dot{e}(t)-K_{AI}e(t)-\eta\,\mathrm{sgn}(S)\\
&+\Delta\nu-\ddot{y}_c+K_{AP}\dot{e}(t)+K_{AI}e(t)\\
&+\frac{1}{r_1}\sum_{j=1}^{M}(\bar{k}_P^j\dot{\bar{k}}_P^j)+\frac{1}{r_2}\sum_{j=1}^{M}(\bar{k}_I^j\dot{\bar{k}}_I^j)\\
=&S^T(-\eta\,\mathrm{sgn}(S)+\Delta\nu)-\frac{1}{r_1}\sum_{j=1}^{M}\left(\bar{k}_P^j\frac{r_1 g_{Pj}S^TS}{\bar{k}_P^j}\mathcal{G}\right) \qquad (20)\\
&-\frac{1}{r_2}\sum_{j=1}^{M}\left(\bar{k}_I^j\frac{r_2 g_{Ij}S^TS}{\bar{k}_I^j}\mathcal{G}\right)\\
\le&\sum_{i=1}^{3}(-\eta|s_i|+l_d|s_i|)-\sum_{j=1}^{M}(g_{Pj}\mathcal{G}S^TS+g_{Ij}\mathcal{G}S^TS).
\end{aligned}
$$

Using the condition that $\eta_i \ge l_d+\ell$, ℓ is an arbitrary positive constant. The previous inequality can be simplified to:

$$
\dot{V}_1 \le -\ell\sum_{i=1}^{3}|s_i|-\sum_{j=1}^{M}(g_{Pj}\mathcal{G}+g_{Ij}\mathcal{G})S^TS\le 0. \qquad (21)
$$

From (18) and (21), it can be known that $V_1(t)$ is positive definite and $\dot{V}(t)$ is non-negative definite. For any $S\in R^3$, $\dot{V}_1\le 0$, then $V_1(t)$ is monotonic decreasing, then $\lim_{t\to\infty}V_1(t)\le V_1(0)$, i.e., $V_1(t)$ is bounded. Then, in view of (21) and Barbalats Lemma [30] and Boundedness Theorem [31] together with (15), the signals K_{AP}, K_{AI} and S are bounded in the closed-loop system.

Next, we will proof the asymptotic convergence of the attitude tracking error e.

Now, consider the following new Lyapunov candidate function:

$$
V_2=\frac{1}{2}S^TS. \qquad (22)
$$

Calculating the time derivative of V_2 yields:

$$
\begin{aligned}
\dot{V}_2 =&S^T\dot{S}\\
=&S^T(\ddot{e}(t)+K_{AP}\dot{e}(t)+K_{AI}e(T)) \qquad (23)\\
=&S^T(\nu+\Delta\nu-\ddot{y}_C+K_{AP}\dot{e}(t)+K_{AI}e(t)).
\end{aligned}
$$

Substituting the controller (17) in (23), one gets:

$$
\begin{aligned}
\dot{V}_2 =&S^T((\ddot{y}_c-K_{AP}\dot{e}(t)-K_{AI}e(t)-\eta\,\mathrm{sgn}(S))\\
&+\Delta\nu-\ddot{y}_c+K_{AP}\dot{e}(t)+K_{AI}e(t)\\
=&S^T(-\eta\,\mathrm{sgn}(S)+\Delta\nu).
\end{aligned}
$$

According to the Assumption 1 and the condition that $\eta_i \ge l_d+\ell$ ($\ell>0$), we can know that:

$$
\begin{aligned}
\dot{V}_2 =&S^T(-\eta\,\mathrm{sgn}(S)+\Delta\nu)\\
\le&\sum_{i=1}^{3}(-\eta|s_i|+l_d|s_i|) \qquad (24)\\
\le&-\ell\sum_{i=1}^{3}|s_i|<0 \qquad \forall S\neq 0.
\end{aligned}
$$

Thus, from (22) and inequality (23), it can be known that $V_2(t)$ is positive definite and $\dot{V}_2(t)$ is negative definite. Therefore, the siding mode manifold S can converge to zero asymptotically.

Once the siding mode manifold $s_i=0$, it follows from (16) that

$$
\dot{e}(t)+\int_0^t K_{AP}\dot{e}(t)+\int_0^t K_{AI}e(t)=0.
$$

Then the dynamic of the closed-loop system can be determined by:

$$
\ddot{e}(t)+K_{AP}\dot{e}(t)+K_{AI}e(t)=0. \qquad (25)
$$

Therefore, it can be concluded that the attitude tracking error converges to zero asymptotically. □

Remark 1: Unlike the PID-type sliding mode control used in [32], the proposed AFPID-SMC adopts new form that the gains of the sliding mode manifold are put into the integral symbol to avoid existing derivative terms of fuzzy parameters in the controller. It should be noticed that this form directly simplifies the solving process and result of the controller.

Remark 2: For the attitude system of reentry vehicle (5), the CPID-type sliding mode manifold is designed as:

$$
S=\dot{e}(t)+K_Pe(t)+K_I\int_0^t e(t)dt.
$$

However, in this paper, the AFPID-type sliding mode manifold $S=[s_1,s_2,s_3]^T$ is designed as follows:

$$
S=\dot{e}(t)+\int_0^t K_{AP}\dot{e}(t)dt+\int_0^t K_{AI}e(t)dt.
$$

We can see that the gains of the sliding mode manifold are put into the integral symbol, so that the derivative of fuzzy term will not appear in the control variable. It should be noticed that this designed method simplifies the solving process and result of the control variable. Besides, the question of the well-posedness of the system equations is avoided during the Lyapunov analyses.

Remark 3: Due to the regulation strategy of the gain parameters of PID-type sliding mode manifold, the problem of the actuator saturation is avoided by setting suitable initial gain values even existing large initial tracking error. But this method cannot guarantee that the system maintain stable when the actuator saturation has occurred. Namely, the proposed controller is not saturation control algorithm. Therefore, it is worthy of consideration for further research.

Remark 4: In practical application, the switching term given in (9) and (17) may result in the control chattering due to imperfections in switching devices. To eliminating the chattering phenomenon, the boundary layer technique is applied in (9) and (17). The saturation function $sat(S) = [sat(s_1), sat(s_2), sat(s_3)]^T$ is used to replace the sign function, and is defined by:

$$sat(s_i) = \begin{cases} \dfrac{s_i}{\bar{\omega}_i} & \text{if } |s_i| < \bar{\omega}_i, \\ \text{sgn}(s_i) & \text{if } |s_i| > \bar{\omega}_i, \end{cases} \quad i = 1,2,3, \tag{26}$$

where $\bar{\omega}_i > 0$ represents the boundary layer thickness.

The attitude tracking errors will not converge to zero but can be expected to converge to some vicinity of the origin rest with the boundary layer thickness $\bar{\omega}_i$.

4.3. Adaptive RBF neural network disturbance observer

The upper bound information of matched disturbance $\Delta\nu$ is known in Assumption 1, but cannot be obtained in the actual system. To ensure the stability of the controlled system, the method is to select a large switching gain, but it will lead to more exquisite chattering. Because of universal approximation property and robustness against environment noise, neural network (NN) is used for solving this problem.

In this subsection, the adaptive RBF neural network disturbance observer is designed to estimate the matched disturbance $\Delta\nu$. Then, the prior knowledge of the matched disturbance upper bound is obtained and the robustness is enhanced.

Based on the universal approximate property, the disturbance $\Delta\nu$ can be expressed as:

$$\begin{aligned} \Delta\nu =& w^T\Theta(x) \\ =& \hat{w}^T\Theta(x) + \varepsilon, \end{aligned} \tag{27}$$

where $\hat{w} = [\hat{w}_1, \hat{w}_2, ..., \hat{w}_n]$ is the adaptive weighting matrix, $w = [w_1, w_2, ..., w_n]$ is ideal weighting matrix. x is input of the NN and ε is an arbitrary approximate constant. The basis function $\Theta(x)$ is given by:

$$\Theta(x) = [\theta_1(x), \theta_2(x), ..., \theta_n(x)]^T, \tag{28}$$

where $\theta_i(x)$ is gauss basis function. And its expression can be described as follows:

$$\theta_i(x) = g\left(\frac{\|x - \rho_i\|^2}{\gamma_i^2}\right), \quad i = 1,2,...,n,$$

where ρ, γ_i are parameters of gauss basis function.

Assumption 2: The parameter ε is an arbitrary approximate constant, and satisfies the condition:

$$\|\varepsilon\| \le \varepsilon_d, \tag{29}$$

where $\varepsilon_d > 0$ is a positive constant.

In this paper, the input parameters of the ARBF neural network are $(e, \dot{e})$, and the adaptive law of weighting matrix $\hat{w}$ is derived by Lyapunov method. Thus, the unknown lumped disturbances estimation can be rewritten as:

$$\Delta\hat{\nu} = \hat{w}^T\Theta(e, \dot{e}). \tag{30}$$

Finally, the new controller and the adaptive algorithm of optimal weighting matrix are designed as follows:

$$\begin{aligned} \nu =& \ddot{y}_c - K_{AP}\dot{e}(t) - K_{AI}e(t) \\ & - \bar{\eta}\,\text{sgn}(S) + \hat{w}^T\Theta(e, \dot{e}), \end{aligned} \tag{31}$$

$$\dot{\hat{w}} = \lambda\Theta S^T, \tag{32}$$

where the parameters $\bar{\eta} > \varepsilon_d$, $\lambda > 0$.

Theorem 2: Consider the reentry vehicle system (5) with the sliding mode manifold defined by equation (17), and the Assumption 2 is satisfied. The adaptive fuzzy sliding mode controller (31) with the adaptive law (16) and (32) can ensure that the attitude tracking error e asymptotically converge to zero.

The proof for Theorem 2 is given in Appendix A.

Remark 5: In this paper, the RBF neural network observer plays a key role. Firstly, the chattering can be restrained by selecting smaller switching gain because of the compensation function of neural network for the external disturbances. Furthermore, the system robustne- ss is enhanced due to the property of NN against external environment noise. It effectively compensates the errors caused by the saturation function in Remark 4.

5. ILLUSTRATIONS AND DISCUSSION

In this section, the simulations of the nonlinear reentry vehicle system in conjunction with the control laws (9), (17), (31) are carried out to validate the performances of the proposed controller.

The aerodynamic model and parameters of 6-DOF mathematic model of reentry vehicle is taken from [33]. The numerical simulation parameters of the reentry vehicle are given by Table 1.

Case A: Comparison of the transient performance of the reentry vehicle between CPID-SMC and AFPID-SMC without matched disturbance $\Delta\nu$.

The controllers (9) and (17) are carried to verify the transient performance of the proposed controller in this simulation. The attitude tracking errors and aerodynamic

Table 1. Numerical simulation parameters.

Parameter name	Value
Initial velocity and attitude	$V(0) = 2800$ m/s, $h(0) = 30$ km
Desired attitude angle	$\alpha_c = 3°$, $\beta_c = 0°$, $\mu_c = 5°$
Parameters in the AFLS	Fuzzy rule number: $M = 25$ Gauss function parameters: $c = 0.5$, $\sigma = 0.03$
Parameters in the neural nework	Order of NN: 3 Initial weight: $\hat{w}_0 = 0.001$ Gauss function parameters: $\rho_i = [-1, -0.5, 0, 0.5, 1]$, $\gamma_i = 7$
Maximum allowable actuator output	$\lvert\delta\rvert = [\lvert\delta_e\rvert, \lvert\delta_a\rvert, \lvert\delta_r\rvert]^T \leq [30°, 30°, 30°]^T$
Saturation function parameters	$\bar{\omega} = [\bar{\omega}_1, \bar{\omega}_2, \bar{\omega}_3]^T = [0.002, 0.002, 0.002]^T$
Switch gains of SMCs	$\eta = [\eta_1, \eta_2, \eta_3]^T = [0.2, 0.05, 0.5]^T$ $\bar{\eta} = [\bar{\eta}_1, e\bar{t}a_2, e\bar{t}a_3]^T = [0.1, 0.02, 0.2]^T$

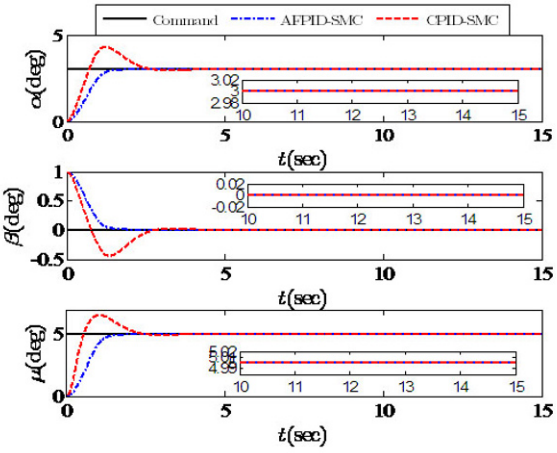

Fig. 3. Simulation results of the attitude tracking of AFPID-SMC and CPID-SMC.

surface deflections are shown in Figs. 3 and 4. From Fig. 3, we can know that the transient performances of the both controllers are dramaticly different. The response speed of system governed by CPID-SMC is faster than that of system governed by AFPID-SMC at the initial phase of control procedure. But the response speed of system governed by AFPID-SMC becomes faster than that of system governed by CPID-SMC with the attitude tracking errors decrease. Additionally, the system governed by CPID-SMC exists response overshoot while the system governed by AFPID-SMC avoids this problem. Therefore, the proposed controller solves the contradiction problem that has been described in the previous section.

In Fig. 4, the aerodynamic surface deflections of the AFPID-SMC are continuous and remain bounded with $|\delta| < 30°$ while CPID-SMC fails fulfill to this constraint.

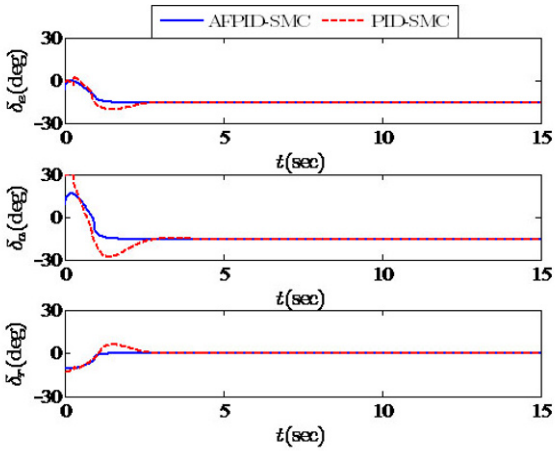

Fig. 4. Simulation results of actuators output of CPID-SMC and AFPID-SMC.

Consequently, the simulation results prove that the problem of the actuator saturation can be avoided under the AFPID-SMC.

The gains of the AFPID-SMC are tuned online by adaptive fuzzy algorithm. From Fig. 5, it is shown that the proportional gain K_{AP} and integral gain K_{AI} are small with the large errors to avoid the saturation of actuator and response overshoot of the system. As errors decrease, the gains become larger and the system response speeds up. Finally, the proportional and integral gains of sliding mode manifold are tuned to ideal values.

Case B: Robustness illustration of AFPID-SMC and comparison of CPID-SMC and AFPID-SMC with matched disturbance $\Delta\nu$.

In order to illustrate the robustness of the AFPID-SMC, and compare the performance of CPID-SMC and AFPID-SMC, we simulate the nonlinear system with external disturbances and modeling inaccuracies.

The aerodynamic characteristic and flight conditions, which tend to change dramatically in the practical application, are taken into consideration. About 10 percent of bias condition for inertia and 20 percent of bias condition for air density are introduced in the simulation scenario.

In addition, the external disturbance torque ΔM is given by:

$$\Delta M = \begin{bmatrix} 1 + \sin(\pi t) + \sin\left(\frac{\pi}{2}t\right) \\ 1 + \sin(\pi t) + \sin\left(\frac{\pi}{2}t\right) \\ 1 + \sin(\pi t) + \sin\left(\frac{\pi}{2}t\right) \end{bmatrix} \times 10^5.$$

1) Robustness illustration of AFPID-SMC

From Section 4, it can be known that the AFPID-SMC is designed for the system with external disturbances and

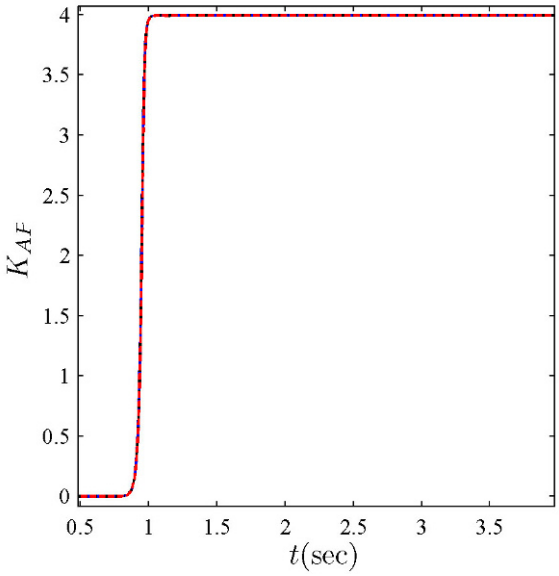

(a) Time-varying proportional gain K_{AP} of AFPID-SMC.

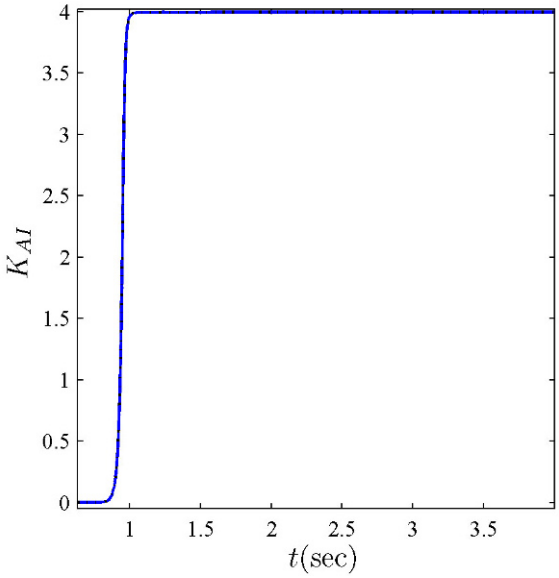

(b) Time-varying integral gain K_{AI} of AFPID-SMC

Fig. 5. Simulation results of the parameters updating online of proposed controller.

modeling inaccuracies. Thus, to illustrate the robustness of the controller, the AFPID-SMC (17) is applied to the actual system. (Atual system represents the model with lumped disturbance $\Delta\nu$, ideal system represents the nominal model.)

The simulation result of the attitude tracking error for ideal and actual system is presented in Fig. 6. And there is no evident difference in effect of attitude tracking errors between actual and ideal system. The system outputs can

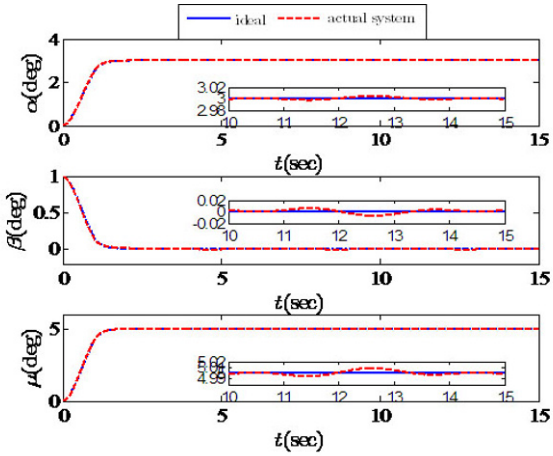

Fig. 6. Effect of the AFPID-SMC on attitude angles tracking of the system with disturbances.

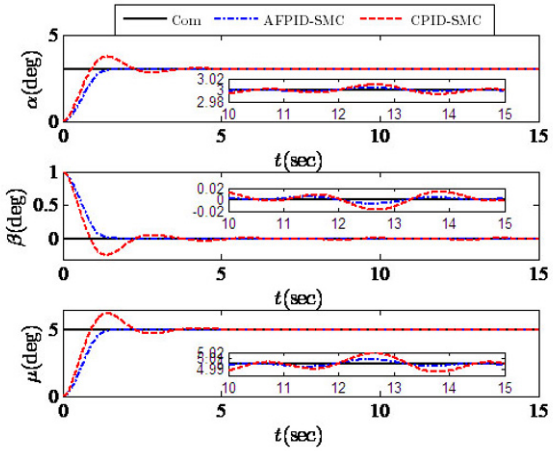

Fig. 7. Comparative results of AFPID-SMC and CPID-SMC.

converge to 1% of their desired values, which verifies the AFPID-SMC robustness against modeling inaccuracies and external disturbances.

2) Comparison of robust performance of the nonlinear system with lumped disturbances $\Delta\nu$ governed by CPID-SMC and AFPID-SMC.

The control laws (9) and (17) are applied to the system with the modeling inaccuracies and external disturbances. The comparisons of the attitude tracking errors are shown for this case in Fig. 7. The outputs of the system governed by AFPID-SMC can converge to 1% of their desired value, it is smaller than that of system governed by PID-SMC, which converges to 2% of the desired value. Thus, it can be seen that AFPID-SMC has better robustness against modeling inaccuracies and external distubances.

Case C: Comparison of robustness of between AFPID-SMC and AFPID-SMC with ARBF neural network distur-

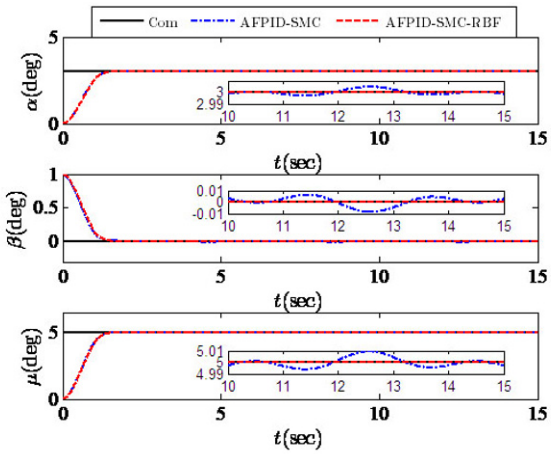

Fig. 8. Simulation results of AFPID-SMC-RBF and AFPID-SMC comparing performance of the robustness of the system.

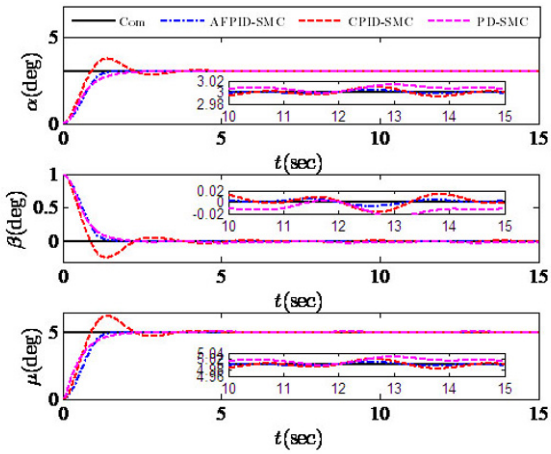

Fig. 9. Simulation results of AFPID-SMC, CPID-SMC and PD-SMC comparing performance of the robustness of the system.

bance observer (AFPID-SMC-RBF) under lumped disturbance Δv.

To compare the robust performance of AFPID-SMC and AFPID-SMC-RBF, about 30 percent of bias condition for inertia and 30 percent of bias condition for air density are considered in the simulation scenario. And the external disturbance torque ΔM becomes 1.2 times initial disturbances.

Fig. 8 presents the results of the attitude tracking errors of the system controlled by AFPID-SMC and AFPID-SMC-RBF. The attitude tracking errors of the system controlled by AFPID-SMC-RBF, that even converging to 1‰, are smaller than that of system contr- olled by AFPID-SMC. So AFPID-SMC-RBF possesses better robustness against modeling inaccuracies and external disturbances, namely, the robustness of AFPID-SMC-RBF is improved due to the usage of RBF neural network.

Case D: Comparison of robustness of between PD (Proportional Derivative)-SMC [12], CPID-SMC and AFPID-SMC.

To shown the transient and robust performances of AFPID-SMC-RBF, about 30 percent of bias condition for inertia and 30 percent of bias condition for air density are considered in the simulation scenario. And the external disturbance torque ΔM becomes 1.2 times initial disturbances.

The PD-SMC is the conventional sliding mode control. To shown the contribution of this paper, the comparison of robustness of between PD-SMC, CPID-SMC and AFPID-SMC is presented in Fig. 9.

Fig. 9 presents the simulation results of the attitude tracking errors of the system. We can see that CPID-SMC is better than PD-SMC in terms of improving the robustness, but the transient performance of PD-SMC is better than that of CPID-SMC. And AFPID-SMC is better than CPID-SMC and PD-SMC in terms of improving the transient performance and robustness.

6. CONCLUSIONS

This study proposes a robust adaptive controller based on adaptive fuzzy logic system and RBF neural network algorithm for reentry vehicle with external disturbances and modeling inaccuracies. The AFPID-SMC adopts adaptive fuzzy algorithm for tuning the gains of sliding mode control online. By designing suitable fuzzy logic system and the adaptive law, the contradiction of the transient and steady state performance of the system is solved. Besides, the problem of actuator saturation is avoided under control input constraint. Furthermore, to enhance the robustness of the reentry vehicle system, the RBF neural network is introduced, which is used to eatimate the unknown lumped disturbances. Finally, the stability of closed-loop system has been achieved by the Lyapunov method with the adaptation mechanisms of the FSL and neural network. The performance of the proposed controller has been examined via numerical simulations.

APPENDIX A

A.1. PROOF OF THEOREM 2

The proof of the Throem 2 is given as follows:

Consider the following Lyapunov candidate function:

$$V_3 = \frac{1}{2}S^T S + \frac{1}{2r_1}\kappa_1\kappa_1^T + \frac{1}{2r_2}\kappa_2\kappa_2^T + \frac{1}{2\lambda}tr(\tilde{w}^T\tilde{w}), \tag{A.1}$$

where $\tilde{w} = w - \hat{w}$, $tr(\cdot)$ is the trace of matrix.

Calculating the time derivative of V_3, and substituting (15) in (A.1), one can obtain:

$$\begin{aligned}\dot{V}_3 =& S^T\dot{S}+\frac{1}{r_1}\dot{\kappa}_1\kappa_1^T+\frac{1}{r_2}\dot{\kappa}_2\kappa_2^T+\frac{1}{\lambda}tr(\tilde{w}^T\dot{\hat{w}})\\ =& S^T(\ddot{e}(t)+K_{AP}\dot{e}(t)+K_{AI}e(t))\\ &-\frac{1}{r_1}\sum_{j=1}^{M}\left(\bar{k}_P^j\frac{r_1 g_{Pj}S^TS}{\bar{k}_P^j}\mathcal{G}\right)\\ &-\frac{1}{r_2}\sum_{j=1}^{M}\left(\bar{k}_I^j\frac{r_2 g_{Ij}S^TS}{\bar{k}_I^j}\mathcal{G}\right)\\ =& S^T(\nu+\Delta\nu-\ddot{y}_c+K_{AP}\dot{e}(t)+K_{AI}e(t))\\ &-\sum_{j=1}^{M}(g_{Pj}\mathcal{G}S^TS+g_{Ij}\mathcal{G}S^TS)-\frac{1}{\lambda}tr(\tilde{w}^T\dot{\hat{w}}). \quad (A.2)\end{aligned}$$

Substituting control expression for (31) in (A.2), one can obtain:

$$\begin{aligned}\dot{V}_3 =& S^T(-\bar{\eta}\,\mathrm{sgn}(S)-\hat{w}^T\Theta(e,\dot{e})+\Delta\nu\\ &-\sum_{j=1}^{M}(g_{Pj}\mathcal{G}S^TS+g_{Ij}\mathcal{G}S^TS)-\frac{1}{\lambda}tr(\tilde{w}^T\dot{\hat{w}})\\ =& S^T(-\bar{\eta}\,\mathrm{sgn}(S)+\tilde{w}^T\Theta(e,\dot{e})\\ &-\sum_{j=1}^{M}(g_{Pj}\mathcal{G}S^TS+g_{Ij}\mathcal{G}S^TS)-\frac{1}{\lambda}tr(\tilde{w}^T,\dot{\hat{w}}) \quad (A.3)\\ =& S^T(-\bar{\eta}\,\mathrm{sgn}(S))-\sum_{j=1}^{M}(g_{Pj}\mathcal{G}S^TS+g_{Ij}\mathcal{G}S^TS)\\ &+S^T\tilde{w}^T\Theta-\frac{1}{\lambda}tr(\tilde{w}^T\dot{\hat{w}}),\end{aligned}$$

where $\tilde{w}$ is the apprpximation error of optimal weighting matrix, and $\Delta\nu = w^T\Theta(e,\dot{e}) = (\hat{w}+\tilde{w})^T\Theta(e,\dot{e})$.

Substituting the adaptive laws (32) in (A.3) and noting that $tr(\tilde{w}^T\Theta S^T) = S^T\tilde{w}^T\Theta$, one can obtain:

$$\begin{aligned}\dot{V}_3 =& -\eta\sum_{i=1}^{3}|s_i|-\sum_{j=1}^{M}(g_{Pj}\mathcal{G}S^TS+g_{Ij}\mathcal{G}S^TS)+S^T\tilde{w}^T\Theta\\ &-\frac{1}{\lambda}tr(\tilde{w}^T\lambda\Theta S^T)\\ =& -\bar{\eta}\sum_{i=1}^{3}|s_i|-\sum_{j=1}^{M}(g_{Pj}\mathcal{G}S^TS+g_{Ij}\mathcal{G}S^TS)+S^T\tilde{w}^T\Theta\\ &-S^T\tilde{w}^T\Theta \quad (A.4)\\ =& -e\bar{t}a\sum_{i=1}^{3}|s_i|-\sum_{j=1}^{M}(g_{Pj}\mathcal{G}+g_{Ij}\mathcal{G})S^TS.\end{aligned}$$

From (A.4), it can be known that $V_3(t)$ is monotonic decreasing, then $\lim_{t\to\infty}V_3(t)\le V_3(0)$, i.e., $V_3(t)$ is bounded. Therefore, the signals κ_1, κ_2 are bounded in the closed-loop system.

The proof of asymptotic stability of the attitude tracking error and the sliding mode manifold is the same as Theorem 1. □

REFERENCES

[1] H. J. Xun, M. D. Mirmirani, and P. A. Ioannou, "Adaptive sliding mode control design for a hypersonic flight vehicle," *Journal of Guidance, Control, and Dynamics*, vol. 27, no. 5, pp. 829-838, 2004. [click]

[2] J. Geng, Y. Z. Sheng, and X. D. Liu, "Finite-time sliding mode attitude control for a reentry vehicle with blended serodynamic surfaces and a reaction control system," *Chinese Journal of Aeronautics*, vol. 27, no. 4, pp.964-976, 2014. [click]

[3] Q. Wang and R. F. Stengel, "Robust nonlinear control of a hypersonic aircraft," *Journal of Guidance, Control, and Dynamics*, vol. 23, no. 4, pp.577-585, 2000. [click]

[4] H. Huang and Z. Zhang, "Characteristic model-based H2/H robust adaptive control during the re-entry of hypersonic cruise vehicles," *Science China Information Sciences*, vol. 58, no. 1, pp. 1-21, January 2015.

[5] Y. Shtessel, J. McDuffie, M. Jackson, and C. Hall, "Sliding mode control of the X-33 vehicle in launch and reentry modes," *Report No.: AIAA-1998-4414*, 1998.

[6] Y. Shtessel, C. Hall, and M. Jackson, "Reusable launch vehicle control in multiple-time-scale sliding modes," *J Guid Control Dyn*, vol. 23, no. 6, pp. 1013-1020, 2000.

[7] T. L. Chung and T. H. Bui, "Sliding mode control of two-wheeled welding mobile robot for tracking smooth curved welding path," *KSME International Journal*, vol. 18, no. 7, pp. 1094-1106, 2004. [click]

[8] N. Hung, T. D. Viet, J. S. Im, and H. K. Kim, "Motion control of an omnidirectional mobile platform for trajectory tracking using an integral sliding mode controller," *International Journal of Control, Automation, and Systems*, vol. 8, no. 6, pp. 1221-1231, 2010.

[9] V. Utkin and J. Shi, "Integral sliding mode in systems operating under uncertainty conditions," *Proc. of the 35th IEEE Conference on Decision and Control*, pp. 4591-4596, 1996.

[10] Q. Zong, J. Wang, and B. L. Tian, "Quasi-continuous high-order sliding mode controller and observer design for flexible hypersonic vehicle," *Aerospace Science and Technology*, vol. 27, no. 1, pp. 127-137, 2013. [click]

[11] X. X. Hu, L. G. Wu, C. H. Hu, and H. J. Gao, "Adaptive sliding mdoe tracking control for a flexible air-breathing hypersonic vehicle," *Journal of The Franklin Institute*, vol. 349, no. 2, pp. 559-577, March 2012. [click]

[12] J. Slotine, "Sliding mode controller design for nonlinear system," *International Journal of Control*, vol. 40, no. 2, pp. 421-434, 1984. [click]

[13] J. Slotine and S. Sastry, "Tracking control of nonlinear systems using sliding surfaces with application to robot manipulator," *International Journal of Control*, vol. 38, no. 2, pp. 465-492, 1983. [click]

[14] T. L. Chern and Y. C. Wu, "Design of integral variable structure controller and application to electronic hydraulic velocity servos systems," *IEEE Proceedings D Control Theory and Applications*, vol. 138, no.5, pp. 439-444, 1991.

[15] Y. M. Li and Q. S. Xu, "Adaptive sliding mode control with perturbation estimation and PID sliding surface for motion tracking of a piezo-driven micromanipulator," *IEEE Transactions on Control Systems Technology*, vol. 18, no. 4, pp. 798-810, July 2010.

[16] D. Cho, Y. Kato, and D. Spliman, "Sliding mode and classical controller in magnetic levitation systems," *IEEE Control System Magazine*, vol. 13, no. 1, pp. 42-48, 1993.

[17] S. Seshagiri and H. Khalil, "On introducing integral action in sliding mode control," *Proc. of the 41th IEEE Conference on Decion and Control*, Las Vegas, Nevada, USA, 2002.

[18] F. Plestan, Y. Shtessel, V. Bregeault, and A. Poznyak. "New methodologies for adaptive sliding mode control," *International Journal of Control*, vol. 83, no. 9, pp. 1907-1919, 2010. [click]

[19] Y. Shtessel, I. Shkolnikov, and A. Levant, "Smooth second-order sliding modes: Missile guidance application," *Automatic*, vol. 43, no. 7, pp. 1470-1480, 2007.

[20] P. L. Lu, C. Gan, and X. D. Liu, "Finite time distributed cooperative attitude control for multiple spacecraft with actuator saturation," *IET Control Theory and Applications*, vol. 8, no. 18, pp. 2186-2198, 2014.

[21] H. Morioka, K. Wada, and A. Sabanovic, "Neural network based chattering free sliding mode control," *Proc. of the 34th SICE Annual Conference*, pp. 1303-1308, 1995.

[22] D. Munoz and D. Sbarbaro, "An adaptive sliding mode controller for a discrete nonlinear system," *IEEE Transactions on Industrial Electronics*, vol. 47, no. 3, pp. 574-481, 2000.

[23] S. J. Huang, K. S. Huang, and K. C. Chiou, "Development and application of a novel radial basis function sliding mode controller," *Mechatronics*, vol. 13, no. 3, pp. 313-329, 2003. [click]

[24] Z. Y. Zhao, M. Tomizuka, and S. Isaka, "Fuzzy gain scheduling of PID controllers," *IEEE Transactions on Systems*, vol. 23, no. 5, pp. 1392-1398, 1993.

[25] W. V. Soest, Q. Chu, and J. Mulder, "Combined feedback linearization an constrained model predictive control for entry," *Journal of Guidance, Control, and Dynamics*, vol. 29, no.2, pp. 427-434, 2006. [click]

[26] H. B. Sun, S. H. Li, and C. Y. Sun, "Finite time integral sliding mode control of hypersonicvehicles," *Nonlinear Dyn.*, vol. 73, no. 1, pp. 229244, 2013.

[27] Y. Stepanenko and Y. Cao, "Variable structure control of robotic manipulator with PID sliding surfaces," *International Journal of Robust and Nonlinear Control*, vol. 8, no. 1, pp. 79-90, 1998.

[28] Z. A. Min and K. D. Kumar, "Adaptive fuzzy fault-tolerant attitude control of spacecraft," *Control Engineering Practice*, vol. 19, no. 1, pp. 10-21, 2011. [click]

[29] L. X. Wang, *Adaptive Fuzzy System and Control: Design and Stability Analysis*, Prentice Hall, Englewood Cliffs, NJ, 1994.

[30] H. K. Khalil, *Nonlinear System*, Vol. 3, Prentice Hall, Upper Saddle River, 2002.

[31] Z. Qu, *Robust Control of Nonlinear Uncertain Systems*, Wiley, New York, 1998.

[32] I. Eker, "Second-order sliding mode control with experimental application," *ISA Transactions*, vol. 49, no. 3, pp. 394-405, 2010.

[33] J. Shaughnessy, S. Pinckney, and J. McMinn, "Hypersonic vehicle simulation model: winged-cone configuration," *NASA Technical Memorandum 102610*, November 1990.

Zhen Jin received the B.S. degree in Control Science and Engineering from Beijing University of Chemistry Technology (BUCT) in 2013. He is now a M.S. candidate at the School of Automation at BIT. His research interests include nonlinear control, adaptive control, sliding mode control.

Jiabin Chen received his Ph.D. degrees from Shanghai Jiaotong University in 1992. He is currently a professor with the School of Automation in BIT. His research interests include high-precision servo control, spacecraft attitude control.

Yongzhi Sheng received his B.S. and M.S. degrees from Beihang University, in 2003 and 2006, respectively, and his Ph.D. degree from the Graduate School of the Second Academy of China Aero-space in 2009. From 2009 to 2011 he did his post doctor research in Beihang Uni-versity. He is currently a lecturer with BIT. His research interests include guid-ance and control design of reentry vehicle.

Xiangdong Liu received his M.S. and Ph.D. degrees from Harbin Institute of Technology (HIT), in 1992 and 1995, respectively. From 1998 to 2000, he did his post doctor research in mechanical postdoctoral research center in HIT. He is currently a professor with the School of Automation in BIT. His research interests include high-precision servo control, spacecraft attitude control, chaos theory.